

Electrically reconfigurable nanophotonic hybrid grating lens array

Ranjith Rajasekharan, Christoph Bay, Qing Dai, Jon Freeman, and Timothy D. Wilkinson

View online: <http://dx.doi.org/10.1063/1.3449130>

View Table of Contents: <http://scitation.aip.org/content/aip/journal/apl/96/23?ver=pdfcov>

Published by the [AIP Publishing](#)

Articles you may be interested in

[Integrated color filter and polarizer based on two-dimensional superimposed nanowire arrays](#)

J. Appl. Phys. **116**, 044314 (2014); 10.1063/1.4891804

[Reconfigurable fabrication of scattering-free polymer network liquid crystal prism/grating/lens](#)

Appl. Phys. Lett. **102**, 161106 (2013); 10.1063/1.4802919

[Fabrication of nanoscale, high throughput, high aspect ratio freestanding gratings](#)

J. Vac. Sci. Technol. B **30**, 06FF03 (2012); 10.1116/1.4755815

[Waveguide array-grating compressors](#)

Appl. Phys. Lett. **87**, 131104 (2005); 10.1063/1.2056578

[Inductively coupled plasma etching for arrayed waveguide gratings fabrication in silica on silicon technology](#)

J. Vac. Sci. Technol. B **20**, 2085 (2002); 10.1116/1.1510528

Electrically reconfigurable nanophotonic hybrid grating lens array

Ranjith Rajasekharan, Christoph Bay, Qing Dai, Jon Freeman, and Timothy D. Wilkinson^{a)}
*Department of Engineering, Centre of Molecular Materials for Photonics and Electronics,
University of Cambridge, 9 J.J. Thomson Avenue, Cambridge CB3 0FA, United Kingdom*

(Received 24 March 2010; accepted 17 May 2010; published online 8 June 2010)

We demonstrate a switchable hybrid grating lens array using a nanophotonic device fabricated from multiwall carbon nanotubes and liquid crystals which combines diffraction, lensing, and dispersion. Diffraction experiments and computer simulations both show clear and well defined diffraction orders in two dimensions with voltage dependent diffraction efficiency. These characteristics enable the device to be used in the fabrication of miniaturized spectrometers and integrated optics. © 2010

A grating consists of a periodic pattern manufactured by mechanical ruling,¹ holography,² lithography,³⁻⁵ or controlled self-assembly.⁶ It is a key element in many applications,⁷⁻⁹ especially in spectrometers where analysis of a sample is done from dispersed wavelengths. The two main optical functions in a conventional spectrometer are dispersion and focusing of incident light. A large number of components are required in such systems and hence they are bulky. To reduce the size and cost of the system, it is essential to minimize the number of components within the system.¹⁰ This can be achieved by combining different optical functions in one element. We combine diffraction, lensing, and dispersion in a nanophotonic device fabricated by combining a nematic liquid crystal (LC) and an array of conducting multiwall carbon nanotubes (CNTs). Since the diameter of a CNT is in the range 10–100 nm, the interaction between the CNT and LC is restricted to the micrometer scale, which is much smaller compared with current LC devices. The CNTs were grown vertically (height 4 μm) and periodically on quartz (or silicon) substrates by plasma enhanced chemical vapor deposition after employing e-beam lithography to a nickel catalyst layer forming an array.¹¹ The device fabricated on the silicon substrate operated in reflective mode and that on the quartz functioned in transmission mode. When an external electric field was applied between top and bottom electrode, the nanotube acted as both a grating element and an electrode site that spawn an electric field profile dictating the refractive index profile within the nanophotonic device and hence forming a hybrid grating lens element (hybrid grating lenslet). The nanophotonic hybrid grating lenslet has an advantage over conventional one-dimensional and two-dimensional (2D) LC gratings¹²⁻¹⁵ that the device combines grating and lensing together in one element. So the diffraction spot size and intensity are variable in Fourier plane with respect to an external voltage which is useful for realizing a miniaturized spectrometer. In this letter, we present experimental and computational results on the diffraction characteristics of the device and also discuss its potential use in a miniaturized spectrometer and an integrated optical system.

Computer simulations were carried out to understand the relationship between the number of CNTs in each group per hybrid grating lenslet and the diffraction efficiency. The

nanotubes were modeled as an intensity grating and LC as a phase grating because CNTs distort the planar aligned LC molecules in their vicinity. Figure 1(a) shows a computationally modeled hybrid grating lens element where the nanotubes act as an intensity grating and LCs as a voltage reconfigurable phase envelope over the nanotubes. The resultant Gaussian like phase profile over a six nanotube group shown

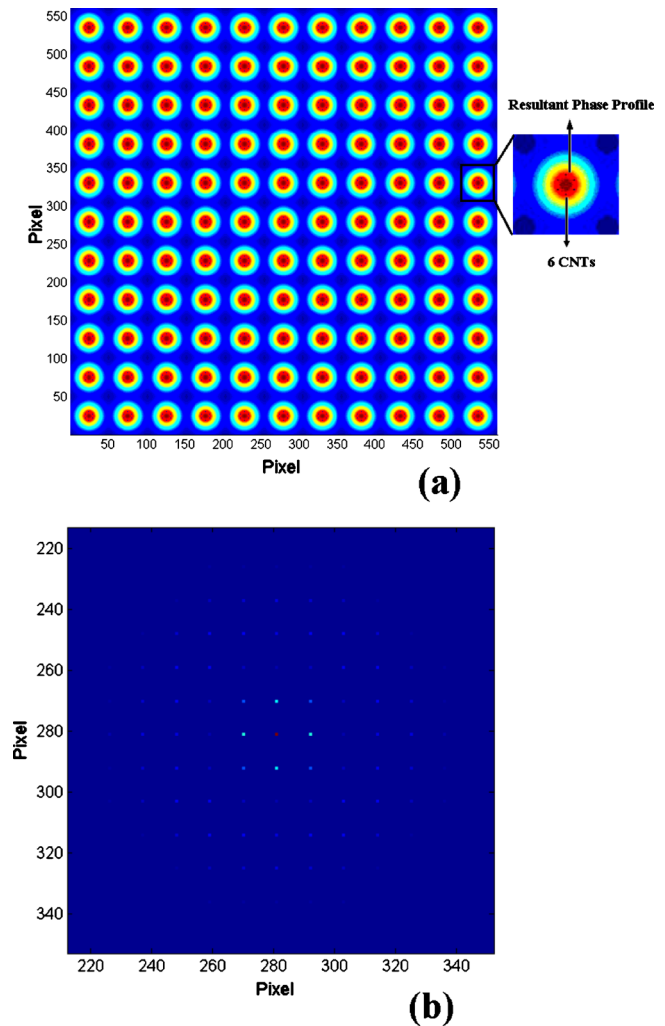


FIG. 1. (Color online) Computationally simulated hybrid grating lens array and diffraction pattern at 1.55 V_{rms} . (a) Each element has six nanotubes (intensity grating) and a resultant phase profile due to LCs (phase grating). (b) Simulated diffraction pattern with center zero order using the hybrid grating lens array model.

^{a)} Author to whom correspondence should be addressed. Electronic mail: tdwl13@cam.ac.uk.

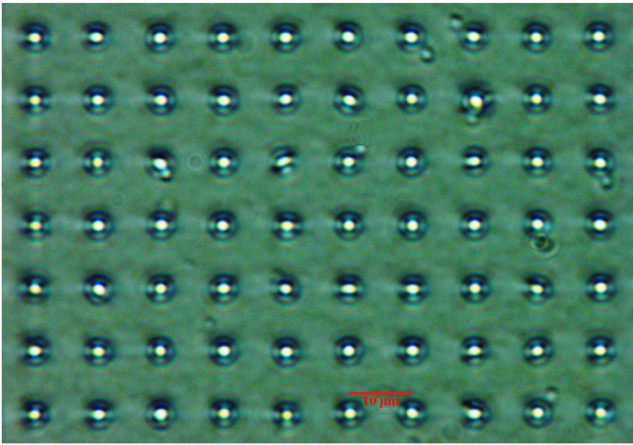


FIG. 2. (Color online) Optical microscope image of a transparent nanophotonic hybrid grating lens array with six nanotubes per each hybrid grating element and a period of $10 \mu\text{m}$ at $1.55 V_{\text{rms}}$ (magnification $50\times$).

in Fig. 1(a) (one element magnified) is due to the combined effect of the Gaussian phase profile over each nanotube in the group. Figure 1(b) shows the simulated diffraction pattern using the simulated intensity and phase grating array. The diffraction pattern consists of a well defined zero order and first orders. The diffraction efficiency was calculated from the simulated diffraction pattern and observed that the diffraction efficiency increased with increase in applied voltage until certain value and then decreased with further increase in applied voltage. This is because of the change in the phase profile and diameter of each hybrid grating lenslet with respect to the applied voltage. The diffraction efficiency was also found to increase with the number of nanotubes per hybrid grating lenslet with a constant periodicity. The computer simulation studies show that the nanophotonic device can be represented as an intensity grating due to the nanotubes and a phase grating due to the LC in the device and that the diffraction efficiency is voltage reconfigurable and increases with the number of nanotubes per group.

Figure 2 shows an optical microscope image of the nanophotonic device with a magnification of $50\times$ at $1.55 V_{\text{rms}}$. The fabricated device has over 1 000 000 hybrid grating lenslets in a $10 \times 10 \text{ mm}^2$ area. The grating period of the nanophotonic device can be increased or decreased further depending upon the application. The diffraction characteristics were studied using the nanophotonic device fabricated on the silicon substrate (reflective device) and the quartz substrate (transparent device). It was found that characteristics of the devices were almost identical. A He-Ne laser with wavelength of 633 nm was used as a source to record the diffraction pattern from the transparent nanophotonic device. The collimated laser beam was incident on the device normal to the surface and diffraction patterns were recorded on a charge coupled device (CCD) camera. The applied voltage to the nanophotonic device was varied from 0 to $7 V_{\text{rms}}$ to study intensity variation in the diffraction patterns and hence diffraction efficiency. Since the incident laser light was perpendicular to the device surface, the diffraction behavior of the device can be determined by the simplified grating equation $m\lambda = d \sin \theta$, where m is the diffraction order, $\lambda(633 \text{ nm})$ the wavelength of the incident light, $d(10 \mu\text{m})$ the period of the nanotubes group, and θ diffraction angle with respect to the grating normal. The dif-

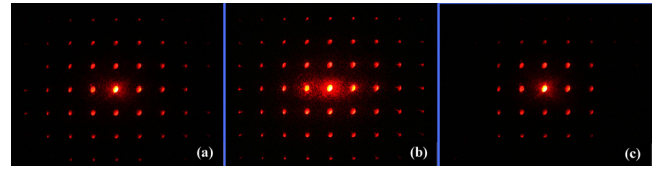


FIG. 3. (Color online) CCD camera images of diffraction patterns generated from the transparent nanophotonic device under He-Ne laser light (633 nm). (a) Diffraction pattern at $0 V_{\text{rms}}$, (b) $1.55 V_{\text{rms}}$, and (c) $6 V_{\text{rms}}$.

fraction angle calculated was 3.63° . Figure 3 shows the diffraction pattern generated from a transparent nanophotonic device with six nanotubes per group which formed a hybrid grating lenslet with a period of $10 \mu\text{m}$ at 0, 1.55, and $6 V_{\text{rms}}$. From the Fig. 3 it is clear that the incident laser beam is diffracted into first orders with a central zeroth order. The zeroth order can be reduced further by individually addressing each hybrid grating lenslet. The intensity of diffraction orders in x axis is found to be slightly greater than in y axis because the LC alignment was along x axis. The diffraction efficiency (DE) of the nanophotonic device was measured using a laser power meter instead of the CCD camera in the experimental setup. The diffraction efficiency device was calculated using the equation $DE = \sum I / I_0$ (Ref. 16) where I is the sum of the intensity in all of the diffracted beams and I_0 is the intensity of the incident beam. The diffraction efficiency was measured as 58% at $0 V_{\text{rms}}$, which then increased to 72% at $1.55 V_{\text{rms}}$ and decreased with further increase in the voltage as shown in Fig. 4(a). We have demonstrated a nanophotonic device with well clear diffraction orders and voltage dependant diffraction efficiency. The increased diffraction efficiency at $1.55 V_{\text{rms}}$ was due to a maximum phase modulation of 4.2π (13.18 radians) of each hybrid grating lenslet of the nanophotonic device as shown in Fig. 4(b). An interference setup was used to recover the

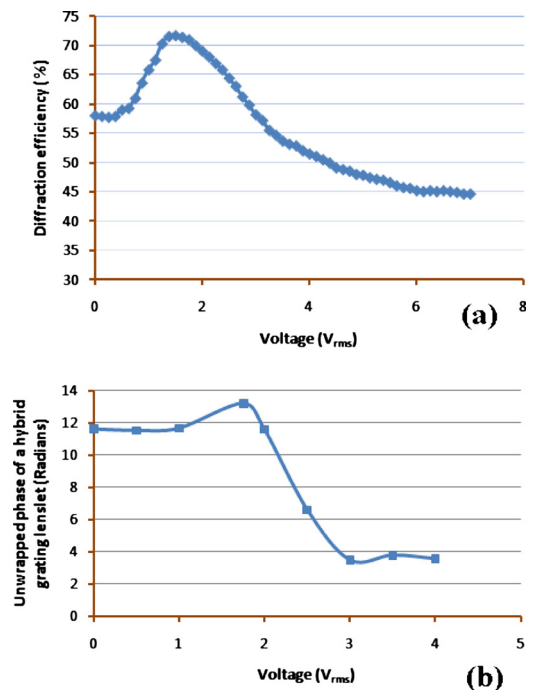


FIG. 4. (Color online) (a) Diffraction efficiency of the transparent nanophotonic device vs applied voltage. (b) Unwrapped phase in radians of one grating lenslet vs applied voltage.

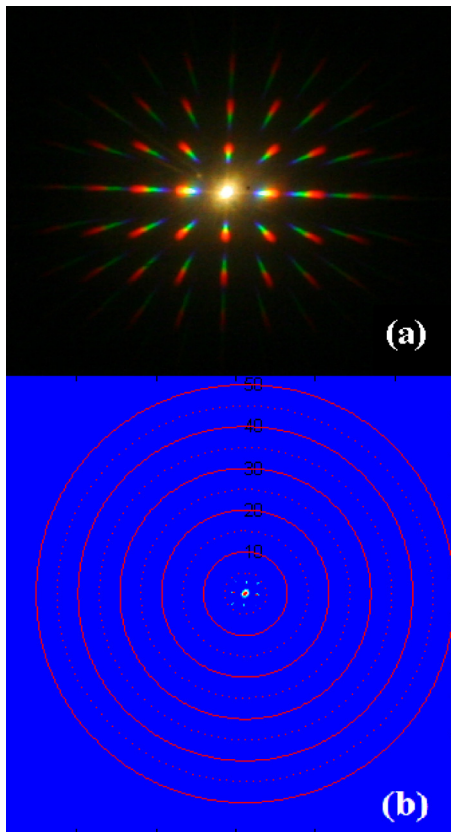


FIG. 5. (Color online) CCD camera images of diffraction patterns generated from the device under white light. (a) Different wavelengths dispersed in the diffraction orders. (b) Experimentally obtained diffraction angle. The circles represent the angle of diffraction. The diffraction angle for first order is 3.7° .

phase profile of each hybrid grating lenslet. The phase modulation of the hybrid grating lenslet is 3.7π at $0 V_{\text{rms}}$ and increased to 4.2π at $1.55 V_{\text{rms}}$. The phase modulation decreased after $1.55 V_{\text{rms}}$ and hence so did the diffraction efficiency. The experiment was then extended to a white light source. When white light was incident on the device, dispersion of different wavelengths in the diffraction pattern was observed in the CCD camera as shown in Fig. 5(a). The measured angle of divergence from the experimental setup was 3.7 degrees for 633 nm as shown in Fig. 5(b) and matches with the calculated value of 3.63° using the grating equation. The focal length of each hybrid grating lenslet was calculated using the equation $f = \Gamma^2 / 2\text{OPD}$ (Ref. 17) where OPD is the peak- to valley- optical path difference from the center to the edge of the hybrid grating lenslet and Γ is the radius of the test area ($5 \mu\text{m}$). The focal length was $10 \mu\text{m}$ at $0 V_{\text{rms}}$ and increased to $35 \mu\text{m}$ at $3 V_{\text{rms}}$. Further increase in the voltage distorted the orientation of LC molecules in the device and hence no focusing observed. The focal length variation was due to the change in phase profile with respect to the applied voltage. The variation in phase profile of each hybrid grating lenslet caused the variation in intensity in the diffraction orders (Fourier space) and hence gave voltage reconfigurable diffraction efficiency. The dispersion combined with the voltage dependant intensity variation in the diffraction orders of the device can be used to align different wavelengths to a respective number of fibers placed just behind the nanophotonic device. This principle can be used to make a miniature spectrometer. In a typical spectrometer optical system 2D images are wavelength fil-

tered with many filters for different wavelengths. But such system is not good for the detection of continuous spectra. In some other designs the wavelength of the light source is scanned by a monochromator. But this system cannot be applied for cases that involve luminescence or wavelength shift. The Fourier transform spectroscopic imaging technique serves as a high performance system but requires both a large optical system and a complicated data conversion. The advantage of realizing a spectrometer based on the nanophotonic device lies in the miniaturization, reduction in the total number of optical components by combining different optical functions in one element, increased resolution and design simplicity. In the nanophotonic device CNTs act as intensity grating while LC creates graded refractive index profile for lensing. The device has over 10^6 grating lenslets in $10 \times 10 \text{ mm}^2$ area. We have used six nanotubes group repeated in $10 \mu\text{m}$ separation (period). The period can be reduced further to increase the resolution. In our proposed spectrometer system white light is incident on a sample under observation and then passed through the nanophotonic device followed to align different wavelengths in the diffraction pattern into respective fibers for further analysis.

In conclusion, we present a hybrid grating lens array using a nanophotonic device which acts as a voltage reconfigurable diffracting, dispersing, and focusing element. A diffraction experiment with white light showed the splitting of different wavelengths in the diffraction pattern of the nanophotonic device. A miniaturized spectrometer has been proposed based on the voltage dependant focal power, diffraction, dispersion, and diffraction efficiency of the device. Further study is in progress by fabricating different nanotube electrode geometries and a pixelated top electrode in the nanophotonic device.

The authors thank Philip Hands, Stephen Morris, Haider Butt, Kanghe James Won, and Damien Gardner for the fruitful discussions. Ranjith specially thanks U.K.-India Education and Research Initiative (UKIERI) and Cambridge Commonwealth Trust (CCT) for giving funding to pursue PhD.

¹G. R. Harrison and E. G. Loewen, *Appl. Opt.* **15**, 1744 (1976).

²D. Rudolph and G. Schmal, *Optik (Stuttgart)* **30**, 475 (1970).

³S. Y. Chou, P. R. Krauss, and P. J. Renstrom, *Science* **85**, 272 (1996).

⁴U. U. Graf, D. T. Jaffe, E. J. Kim, J. H. Lacy, H. Ling, J. T. Moore, and G. Rebeiz, *Appl. Opt.* **33**, 96 (1994).

⁵Z. Yu and S. Y. Chou, *Nano Lett.* **4**, 341 (2004).

⁶Z. W. Pan, S. M. Mahurin, S. Dai, and D. H. Lowndes, *Nano Lett.* **5**, 723 (2005).

⁷X. Zhang, L. Hongmei, J. Tian, Y. Song, and L. Wang, *Nano Lett.* **8**, 2653 (2008).

⁸H. Tamada, T. Doumuki, T. Yamaguchi, and S. Matsumoto, *Opt. Lett.* **22**, 419 (1997).

⁹E. Bruce, *IEEE Spectrum* **39**, 35 (2002).

¹⁰S. Traut and H. P. Herzig, *Opt. Eng. (Bellingham)* **39**, 290 (2000).

¹¹T. D. Wilkinson, X. Wang, K. B. K. Teo, and W. I. Milne, *Adv. Mater.* **20**, 363 (2008).

¹²H. Choi, J. W. Wu, H. J. Chang, and B. Park, *Appl. Phys. Lett.* **88**, 021905 (2006).

¹³J. Chen, P. J. Bos, H. Vithana, and D. L. Johnson, *Appl. Phys. Lett.* **67**, 2588 (1995).

¹⁴C. Provenzano, P. Pagliusi, and G. Cipparrone, *Opt. Express* **15**, 5872 (2007).

¹⁵S.-T. Wu and A. Y.-G. Fuh, *Jpn. J. Appl. Phys., Part 1* **43**, 7077 (2004).

¹⁶M. D. Fayer, *Annu. Rev. Phys. Chem.* **33**, 63 (1982).

¹⁷R. Rajasekharan-Unnithan, H. Butt, and T. D. Wilkinson, *Opt. Lett.* **34**, 1237 (2009).